AFRL-AFOSR-VA-TR-2022-0695

Non-local Quantum Interactions Using Trapped Ions and Integrated Photonics

Waks, Edo
MARYLAND UNIV COLLEGE PARK
230 W 41ST STREET FL 7
NEW YORK, NY,
US

09/29/2022
Final Technical Report

DISTRIBUTION A: Distribution approved for public release.

Air Force Research Laboratory
Air Force Office of Scientific Research
Arlington, Virginia 22203
Air Force Materiel Command

REPORT DOCUMENTATION PAGE

PLEASE DO NOT RETURN YOUR FORM TO THE ABOVE ORGANIZATION.

1. REPORT DATE	2. REPORT TYPE	3. DATES COVERED	
20220929	Final	START DATE 20160930	END DATE 20210929

4. TITLE AND SUBTITLE
Non-local Quantum Interactions Using Trapped Ions and Integrated Photonics

5a. CONTRACT NUMBER	5b. GRANT NUMBER	5c. PROGRAM ELEMENT NUMBER
FA9550-16-1-0421		61102F
5d. PROJECT NUMBER	**5e. TASK NUMBER**	**5f. WORK UNIT NUMBER**

6. AUTHOR(S)
Edo Waks

7. PERFORMING ORGANIZATION NAME(S) AND ADDRESS(ES)
MARYLAND UNIV COLLEGE PARK
230 W 41ST STREET FL 7
NEW YORK, NY
US

8. PERFORMING ORGANIZATION REPORT NUMBER

9. SPONSORING/MONITORING AGENCY NAME(S) AND ADDRESS(ES)	10. SPONSOR/MONITOR'S ACRONYM(S)	11. SPONSOR/MONITOR'S REPORT NUMBER(S)
Air Force Office of Scientific Research 875 N. Randolph St. Room 3112 Arlington, VA 22203	AFRL/AFOSR RTB1	AFRL-AFOSR-VA-TR-2022-0695

12. DISTRIBUTION/AVAILABILITY STATEMENT
A Distribution Unlimited: PB Public Release

13. SUPPLEMENTARY NOTES

14. ABSTRACT
Trapped ions are the leading qubit system for quantum information processing. They possess both long coherence times and high-fidelity two-qubit Coulomb gates between all ions in the trap. They are also ideal sources of indistinguishable photons that can be entangled with quantum memory, which is essential for distributing quantum coherence. But processing these photons with high efficiency and fidelity remains a key challenge in quantum information. Integrated photonic structures are uniquely suited for this application because they combine many tunable components on a compact semiconductor chip, enabling complex photonic circuits that are unattainable using free-space optics. These circuits can apply unitary operations to photons emitted from many ions, opening up the possibility to study quantum physics on a completely new scale. Nevertheless, the integration of trapped ions with photonics integrated circuits remains largely unexplored. In this proposal we will combined trapped ions with integrated photonics to create large-scale quantum photonic circuits. We will co-trap multiple ion species in the same trap to create both stable quantum memory and efficient photon emission. We will couple emitted photons to integrated photonic circuits based on SiN, a low-loss optical material with a high index of refraction. We will use these
circuits to study quantum random walks of multiple photons in a photonic circuit, which have important applications in quantum search, boson sampling, and studying localization effects. We will also use photonic circuits to mediate long-range interactions between many trapped ions to generate large-scale non-local entanglement. The use of quantum random walks to distribute entanglement is largely unexplored and could play an important role in quantum networks and quantum computers. This program will have a strong impact on the capabilities of the air force, and we will transition our devices and expertise in photonics and trapped ions to support the ongoing work of ARL.

15. SUBJECT TERMS

16. SECURITY CLASSIFICATION OF:			17. LIMITATION OF ABSTRACT	18. NUMBER OF PAGES
a. REPORT	b. ABSTRACT	c. THIS PAGE		
U	U	U	UU	2

19a. NAME OF RESPONSIBLE PERSON	19b. PHONE NUMBER *(Include area code)*
GRACE METCALFE	(703) 696-9740

Accomplishments

Research Objectives:
The objectives of this program were to study protocols in the remote entanglement of trapped atomic ions while investigating the use of integrated photonic devices in order to scalably distribute entanglement and scale up the trapped ion quantum computer. We continued the evolution of increased light collection in macroscopic ion traps and discrete high NA objectives to study and optimize photonic protocols. We also developed integrated photonic devices that apply complex unitary operations to multi-photon states generated by ions. These unitary operations enable a broad range of applications in quantum information. Our work also focuses on performing quantum frequency conversion to make the photons emitted by trapped ions compatible with foundry-fabricated Si photonics. This approach enables us to implement a broad range of scalable photonic circuits that can scalably mediate entanglement distribution.

Accomplishments during reporting period:
A detailed list of results including figures is provided in the technical report at the end. Below we summarize major results.

- We developed a polarization independent photonic interconnect to mediate entanglement between trapped ions. The interconnects implement a photonic Bell measurement on photons entangled with ion memory, the key quantum operation required to transmit entanglement over long distances.
- Developed rare-earth ion quantum memories for routing quantum information between ion trap quantum computers. Memories enable buffering of photonic qubits to provide time for switching between different nodes.
- Implemented quantum frequency conversion of trapped ions to telecom for long distance quantum communication

How were the results disseminated to communities of interest:

Results were disseminated through journal and conference publications.

Impacts

Development of the principal discipline(s) of the project:

Optical interconnects are essential to both scale up the ion trap quantum computer and achieve large-scale quantum networks. The technology to interconnect quantum computers is still significantly lacking, and requires innovation in the fields of photonics, nonlinear optics, and atomic physics. This project made significant progress towards that goal by establishing the core physics and technology to achieve scalable quantum interconnects.

Other disciplines:

The devices developed in this project also have clear application in other disciplines. The integrated photonic devices we developed will be extremely useful for optical communications where polarization acts as an additional mode to transmit information. Nonlinear frequency conversion is also an essential tool in nonlinear optics and has many applications for generating light sources at wavelengths that cannot be provided by conventional gain materials.

Describe the impact in this reporting period on the development of human resources:

This project funded multiple students and postdocs who attained experience and skills in the areas of quantum optics, quantum information, integrated photonics, and nonlinear optics. Youngmin Kim took on a faculty position at Colorado Mesa University.

Describe the impact on teaching and educational experiences:

None to report

Describe the impact in this reporting period on physical, institutional, and information resources that form infrastructure:

This project established new facilities in the Physical Sciences Complex for quantum networking and interconnection of trapped ions.

Impact on society beyond science and technology:

None to report.

Changes

Changes in approach:

None to report

Problems or delays:

The COVID pandemic caused a delay in our research due to shutdown of our labs and the cleanroom facilities.

Expenditure Impacts

None to report

Technical Updates

A. Device design

A critical component of optical interconnects for ion trap integration is a polarization independent beamsplitter. These beamsplitters swap entanglement between ions and photons to mediate long-distance ion entanglement. To develop this component, we began with an on-chip directional coupler design, illustrated in Figure 1. We found that a symmetric square waveguide cross-section attains optimal performance. To achieve polarization independent beamsplitting, we numerically optimized the device based on the width, gap and cross section. Figure 1 shows the splitting ratio mismatch as a function of gap and width. From this figure we observe a broad range of device designs that attain polarization independent beamsplitting. The optimized device achieves nearly negligible mismatch in beamsplitting, demonstrating that an on-chip beamsplitter can attain polarization independence.

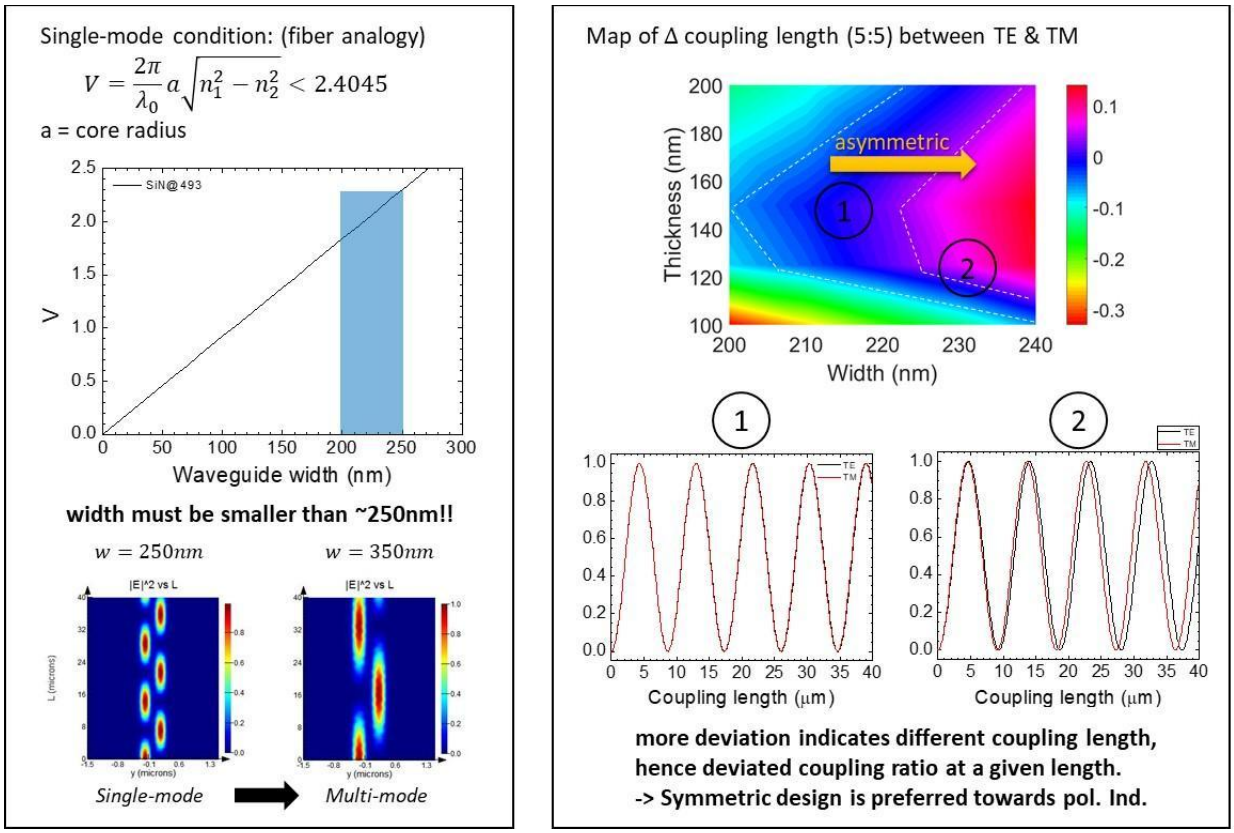

Figure 1: Design of polarization-independent directional coupler. Left panel shows design criteria where we optimize the waveguide geometry to attain single mode operation. Right panel shows coupling mismatch as a function of thickness and width. Blue region identified as region 1 exhibits nearly perfect beamsplitting with no mismatch. Bottom figures show oscillations for both polarizations, showing good beamsplitting behavior over a broad parameter range.

B. Fabrication and testing.

To fabricate the devices, we developed a metal liftoff technique. We began with a sample composed of 200 nm of SiN on top of a thick layer of SiO_2. We grow the SiN using LPCV which produced a highly

uniform SiN layer with low impurities. We used a positive resist (ZEP520) and electron beam lithography to pattern the waveguide structures on top of the chip. We then deposit chrome and perform liftoff in order to produce a hard metal mask for etching. Inductively coupled plasma etching then transfers the mask pattern to the substrate to create the waveguides. We deposit SiO_2 on the fabricated structure in order to create a SiN waveguide fully encased in SiO_2, resulting in a nearly perfectly symmetric structure. Figure 2 shows a fabricated final device.

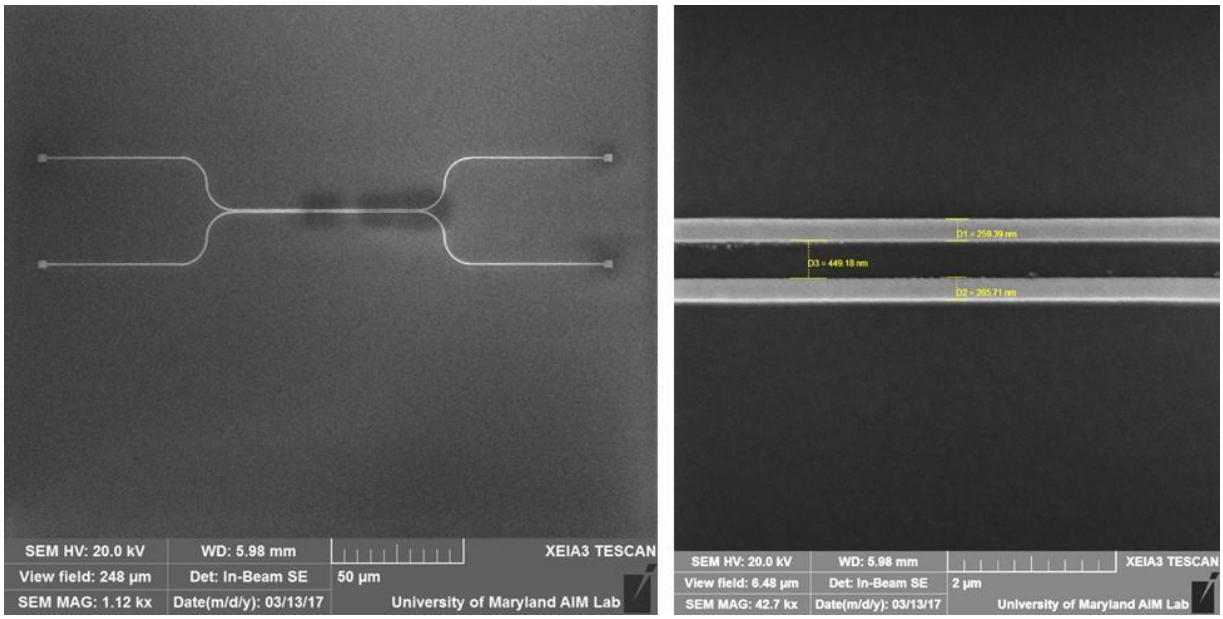

Figure 2: Fabricated directional couplers. Left panel shows a wide field of view, while the right panel shows a closeup of the gap illustrating the accuracy of the fabrication approach. The width and gap of the structure are well-matched to the optimal design.

We developed a mobile testing platform that enables us to rapidly prototype and test devices. This platform can characterize the performance of prototype devices. Once we find a suitable device, we can move the platform to various ion trap labs where we can immediately couple trapped ion emission. This approach has the advantage that we can leverage the many ion traps available at UMD to rapidly perform experiments. Figure 3 shows a picture of the testing platform along with illustrated beamlines. The camera images show characterization results of a fabricated device. The picture in the middle right shows the whole device, where the input beam at the bottom couples to a beamsplitter resulting into two output spots at the top of the image. The top image is a spatially filtered version where we block out the input, isolating the two output ports of the beamsplitter.

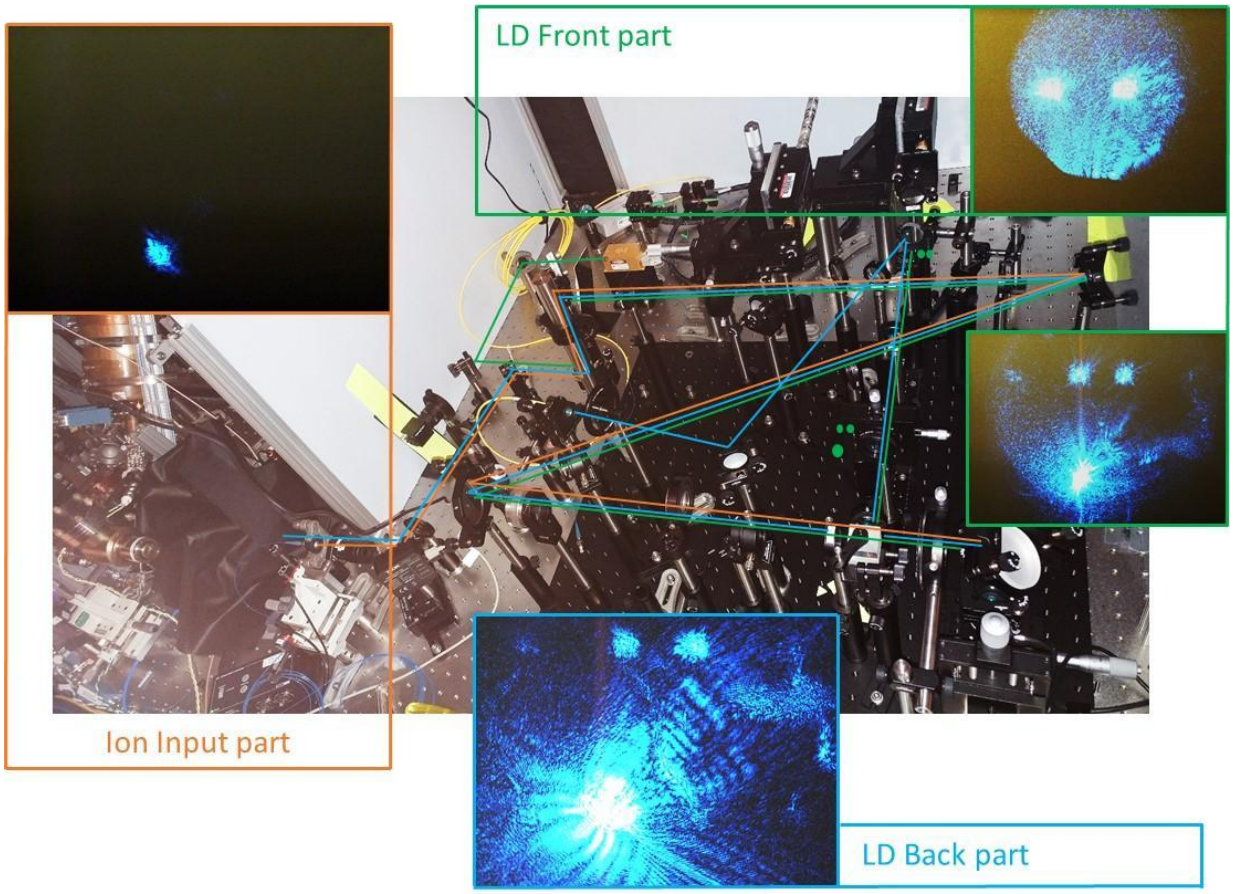

Figure 3: Testing setup for photonic chips. Camera images show characterization of a functioning on-chip beamsplitter. Left image shows the input spot at the bottom, and two output spots. Top left image shows the spatially filtered signal where the input beam is blocked out by an iris.

We have already successfully coupled ion emission to the system. The key challenge was to perform alignment. We developed a unique alignment approach where we illuminate signal from the output gratings and couple the light back to the ion. By time reversal symmetry, the ion emission will then optimally couple to the device.

C. Development of ion trap

We have begun constructing a fully dedicated barium ion trap system. The setup will enable us to trap multiple barium ions and couple the emission into photonic chips. This ion trap will be located in the Waks lab within the pFC. We expect this system to come into operation in the next month. In the meantime, we are using the barium ion traps in the Monroe labs to perform preliminary ion-photonic measurements.

A. Design and Fabrication of polarization-insensitive directional coupler

We optimized designs for photonic devices involving a few dielectric materials (SiN, AlOx, LN) using FDTD simulation tools. Figure 1 shows a summary of simulation results based on silicon nitride as the material of choice. Figure 1a shows a single mode profile of the coupling regime in

a directional coupler. Physical parameters such as the width, height and gap distance are varied to obtain a minimum point between towards polarization-insensitive path as shown in Figure 1c and 1d.

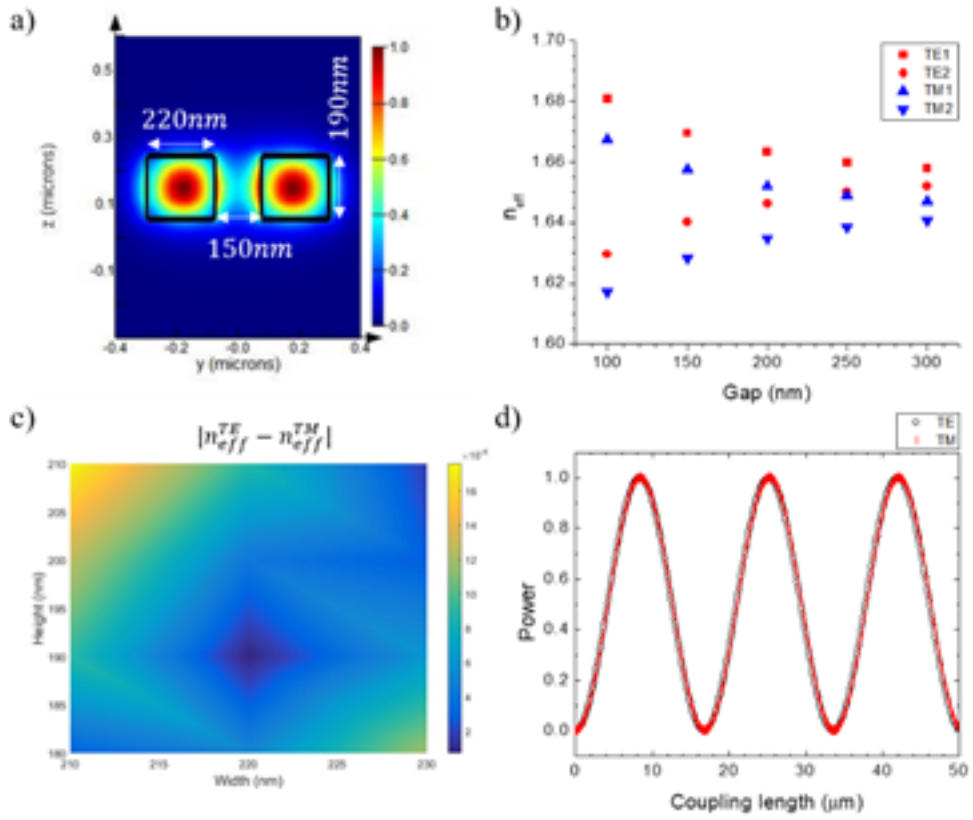

Figure 1: Simulation results on the polarization-insensitivity. a) FDTD mode profile of the coupling regime in a directional coupler with given physical dimensions as shown. b) Calculated effective refractive index of the TE even (red square) and the TE odd (circle) mode versus the separation between the two waveguides. Blue triangles are that of the TM mode. c) A map of effective index differences between TE and TM with varying width and height at a fixed separation distance of 150 nm. The local minimum at width=220 nm; height=190 nm represents a polarization-insensitive region. d) Power oscillation curves for both TE (black) and TM (red) mode along the coupling length direction. Power 0.5 represents 50/50 splitting ratio. The in-phase characteristic between TE and TM shows polarization-insensitive nature of our device.

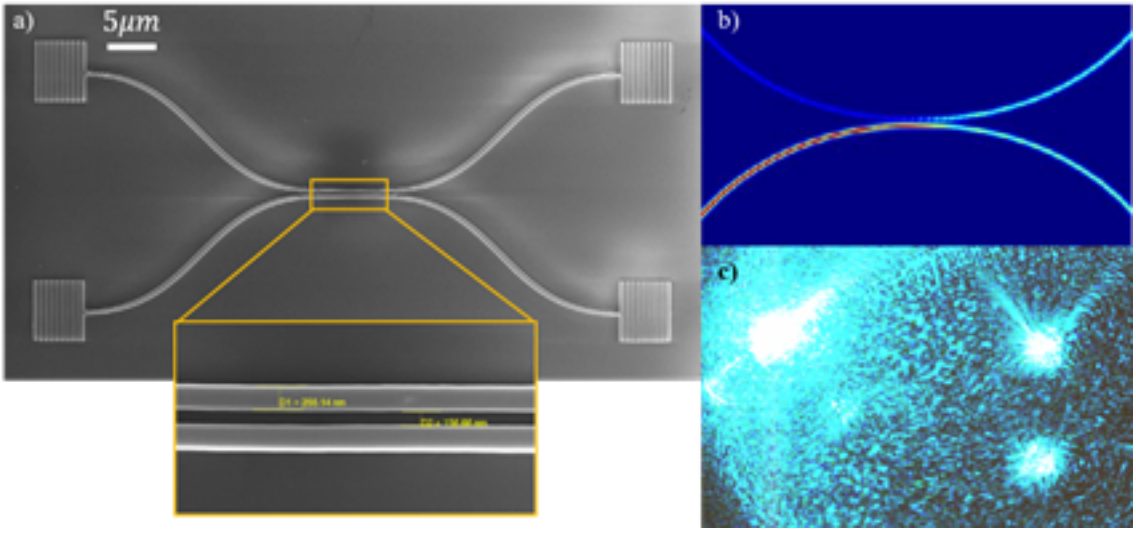

Figure 2: a) SEM images of fabricated devices. b) FDTD simulation of power distribution (blue) showing 50/50 splitting ratio at a calculated coupling length. c) CCD camera images obtained from characterizing the device. Grating couplers are attached on both ends to convert the directionality of the light.

Once the optimized parameters were chosen, we fabricated devices on Si/SiO2/SiN wafers. A few hundred nano-meter thickness of silicon nitride is deposited using LPCVD on thermal oxide layer of 2 um. Structures are then defined via electron beam lithography and subsequently etched via reactive ion etching process. Figure 2a shows SEM images of a fabricated device. Cr shadow masks are used for etching to ensure high sidewall quality. Figure 2b shows a 50/50 power distribution on FDTD simulation. Figure 3c is a CCD camera image obtained from characterizing the device in our optical setup. Square-like grating couplers are added on both ends to convert the directionality of light from out-of-plane to in-plane, and vice versa.

B. Constructing an integrated optical setup with ion-trap chamber system

We constructed an integrated optical setup to combine with the ion-trap system in a single measurement setup. The left image shows an overview structure. The signal from the ion chamber is aligned unto the device using time-reversal technique. The right-hand image shows the right-side of the setup in the left in more detail. It is designed to characterize the polarization measurement using two sets of half-wave plates and polarizers on both input and output path of light.
respectively.

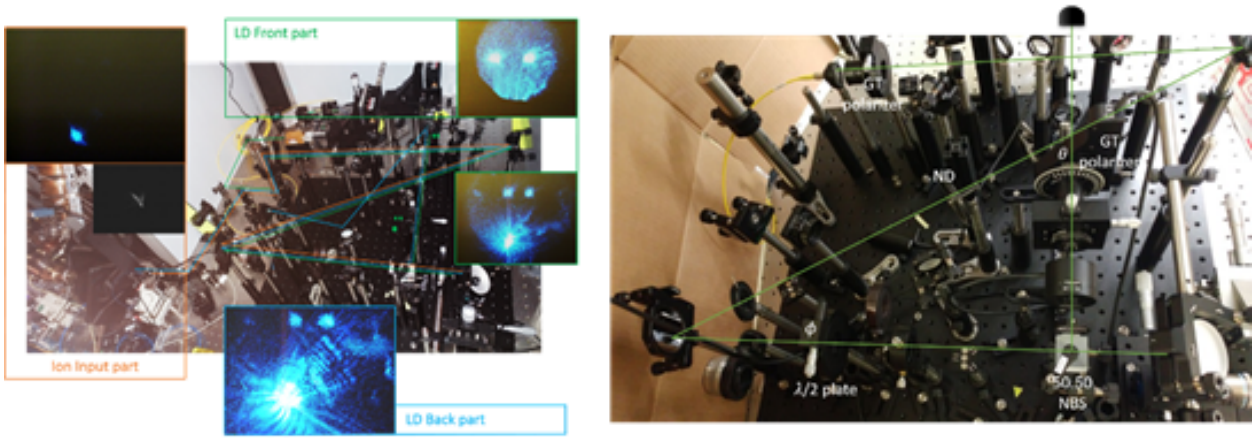

Figure 3: Optical setup images. Left image is an overview of the two integrated system. The photon signals from the left-hand side are aligned onto the device using time-reversal technique. Right is polarization-insensitivity measurement setup. Two half-wave plates are inserted for controlling the input and output polarization, polarizer and analyzer,

C. Construction of a new ion-trap chamber

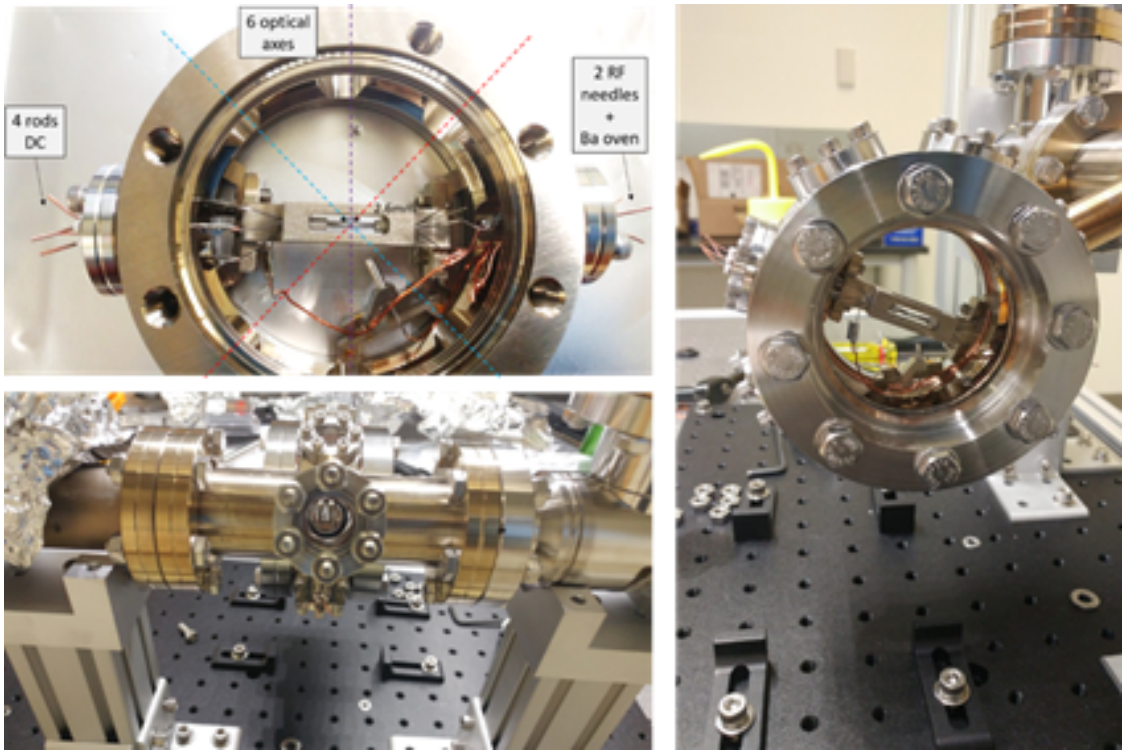

Figure 4: Ion-trap construction images.

We are constructing a new Paul-trap based ion-trap which can host both Yb and Ba simultaneously. Specially designed re-entrant windows are AR-coated at 369, 493 and 650 nm to

be compatible with both Yb and Ba. The Paul trap consists of four-rod dc channels and two rf channels. Assembling is mostly complete.

Our team has been working on optical interconnects for trapped ion quantum computers both at the local data center level and for long distance quantum networks. We have been undertaking the following research tasks:

Reconfigurable UV photonics: We have been working to design, fabricate, and test high quality visible and near UV integrated photonics for interconnecting trapped ions at data center length scales. These photonics enable fast reconfigurable interconnection of trapped ions by integrating many photonic Bell-state analyzers on a compact chip. Our effort has focused on MgO doped lithium niobate which exhibits high transparency in the visible and UV wavelengths. We have fabricated various integrated photonic structures and have also performed a design of compact on-chip Bell analyzers. In addition, we have designed improved coupling methods that increase photon coupling efficiency into the chip, a critical requirement.

Quantum frequency conversion: Ions emit at UV to visible wavelengths which are not suitable for fiber based optical networks. We are working on QFC of Ba ions for ion trap based quantum networks.

Optical quantum memories: Scalable networks require efficient storage of photons for quantum interconnection. We are working on integrated photonic optical quantum memories that can store photons for quantum networking applications. To this end, we have developed a new material, rare-earth ion doped thin-film lithium niobate.

Below we provide a detailed update of the above research thrusts.

UV Photonics

Fabrication of Near UV photonics: To overcome the limitation of the metal lift process, we use negative resist and use the resist as a mask layer to etch and pattern rare earth doped thin film lithium niobate. We have developed a new recipe which is shown below.

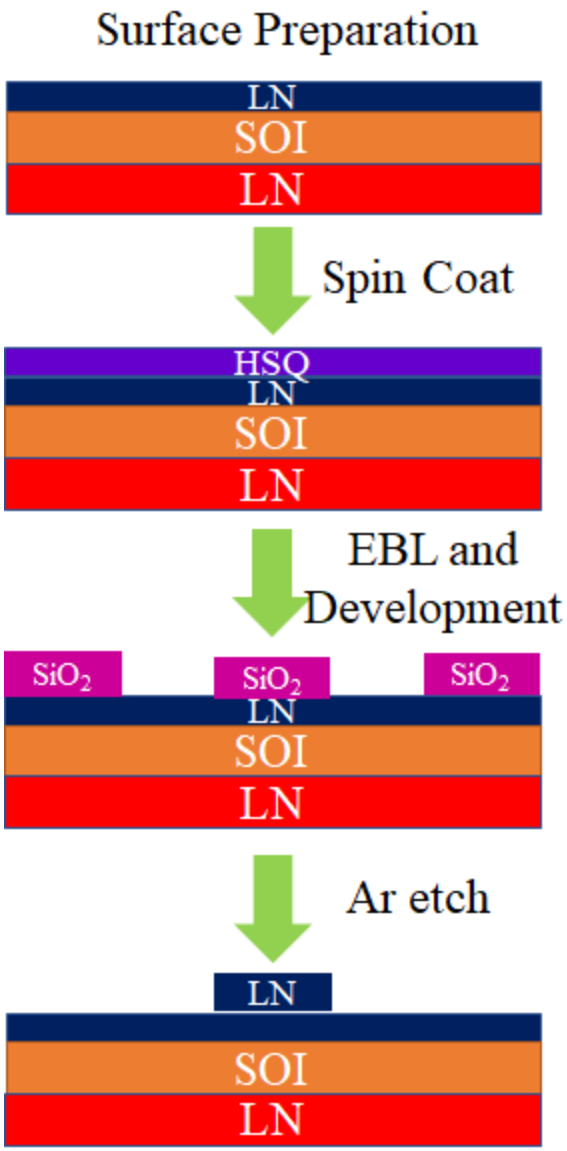

In this recipe, we are cleaning the rare earth doped lithium niobate chips with acetone and isopropyl alcohol for 5 mins respectively . To remove organic substances, we are doing oxygen plasma cleaning for 3 mins with 200 W power and 100 scum pressure on the trion etcher. We are using hydrogen silsesquioxane (Fox 16 provided by Dow) as our negative electron beam lithography resist. For the adhesion of Fox 16, we are prebaking the chips on a hot plate for 5 mins at 225℃. Following the prebaking, we are then spinning the Fox16 at 2000 rpm for 1 mins which deposits 600 nm of hydrogen silsesquioxane. For high resolution structures, we are baking our chips for 4 mins at 80℃ temperature. Currently, we have been successful to deposit 60 nm width of line with an aspect ratio of 10 which might be crucial for developing nanophotonics devices. To avoid charging issues in electron beam exposure we are using AQUASAVE which is spin coated for 45 secs at 4000 rpm on our chips. We are then using electron beam of 1 nA

writing current, 3000 microC/cm2 to pattern our devices. To remove the AQUASAVE, we are dipping our exposed chips into water for 1 mins. After developing with 25% TMAH at 50 degrees celsius, we are using argon plasma etching for transferring our structure to thin film lithium niobate. Currently, we are optimizing the etching process for minimizing the surface roughness of the waveguides to achieve low losses at 493 nm wavelength. The figure below shows the SEM images of the directional coupler, grating coupler that we have fabricated through our current recipe.

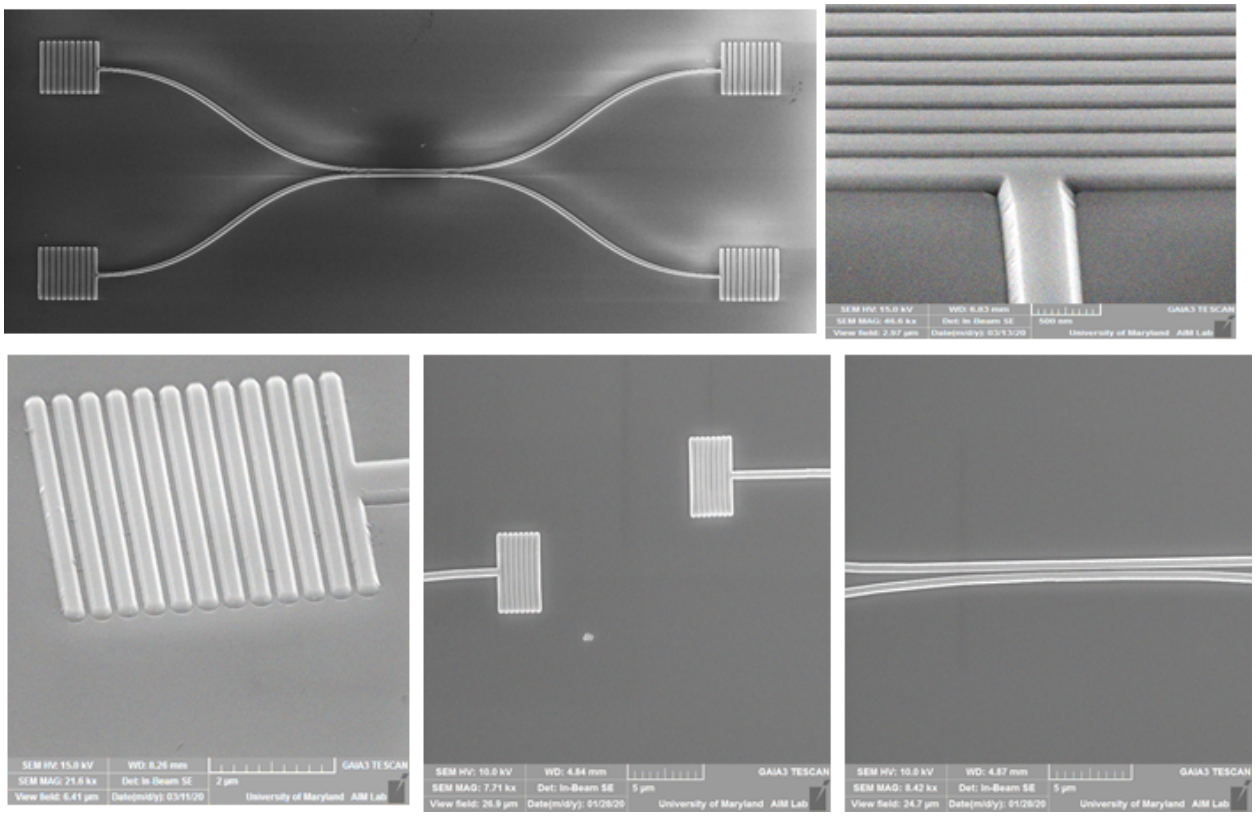

Figure. SEM images of directional coupler, grating coupler and coupling regions of near UV ring resonators with our current recipe.

Lithium niobate photonic Bell analyzers

The possibility of transmitting quantum states encoded in a photon through fiber optic network and the advances in nonlinear optics which enables the generation of single and entangled photons make integrated photonics the key for large scale quantum computation and communication. In this respect, lithium niobate has been attractive platform for its broad transparency window from 350 nm to 2500 nm wavelength, high electro optic coefficient, second order nonlinearities, piezoelectric and pyroelectric properties, and its ability to be phase matched through periodic poling. Recent progress in dry etching has enabled the development of thin film lithium niobate materials achieving high index contrast, which allows for scalable photonic devices. However, polarization independent directional coupler hasn't been realized in lithium

niobate platform limiting its application in integrated photonics. Quantum information of barium ions can be entangled in the polarization degree of freedom of single photons. Therefore, achieving polarization independent optical switches and couplers are essential for wide spread quantum communication in ion photonics. For that reason, we have designed a polarization independent directional coupler in lithium niobate to achieve an optical interface for quantum interconnect between distant ion traps.

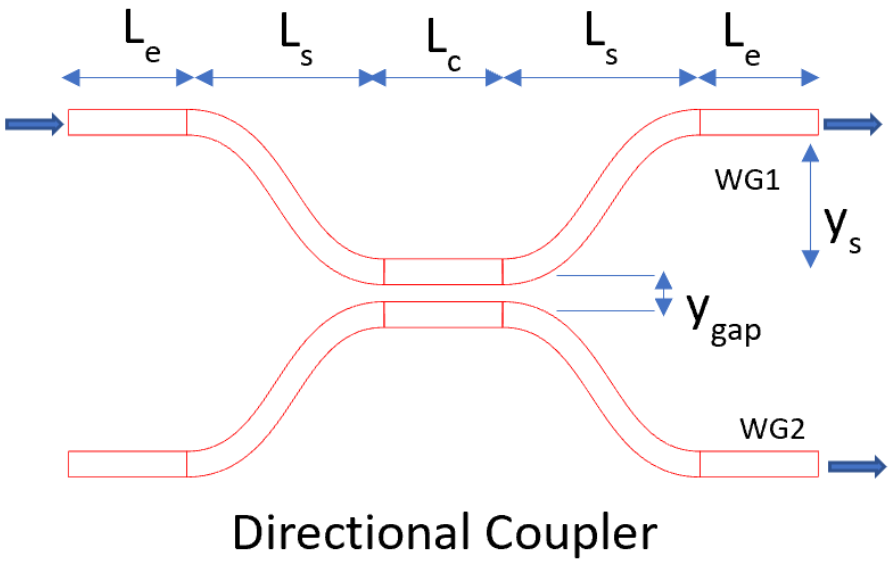

Fig. 1 2-D schematic of the polarization insensitive directional coupler.

Fig. 1 represents the schematic of the directional coupler used in our simulation. In our design, we have used rib waveguide structure to minimize the scattering losses from side wall roughness. We have designed on 300 nm thin film single crystalline lithium niobate on the top of 2 microns thick SiO_2 supported by single crystal lithium niobate substrate which is commercial available by NanoLN. We have considered the sidewall angle of 75 degrees in our design reported by Krasnokutska et al. (Opt. Express 26, 897-904 (2018)). Side angle due to imperfect vertical etching and device asymmetry because of rib waveguide structure makes difficult for polarization insensitive coupler in lithium niobate. For that reason, we have optimized the etching depth, width, bending length, gap, coupling length of directional coupler to achieve polarization independent 50-50 splitting ratio.

According to mode couple theory, we can classify the modes of the directional coupler into symmetric and antisymmetric modes and the power splitting ratio of the directional coupler depends on the difference of effective refractive index of the symmetric and asymmetric mode. Therefore, we can achieve a polarization independent power splitting ratio by making the index contrast of the even and odd modes equal for the transverse electric (TE) and transverse magnetic (TM) modes. We definFig. 2 (a) Variation of Δn_TE-Δn_TM with respect to width and

etch depth of directional coupler. (b) The symmetric (c) and antisymmetric modes of the directional coupler for TE polarization and for index contrast of symmetric and antisymmetric modes for TE and TM polarization. We have tried to minimize by varying the width and etch depth of the waveguide (Fig. 2(a)). Within the single mode region indicated by red line in Fig. 2 (a) we found the minimize index contrast for the TE and TM modes at a height of 120 nm and width of 600 nm. Fig 2. (b) and (c) represent the symmetric and antisymmetric mode for TE polarization respectively. In these simulations, we have considered 75 nm gap between the waveguides which yields the minimum index contrast for achieving polarization independence.

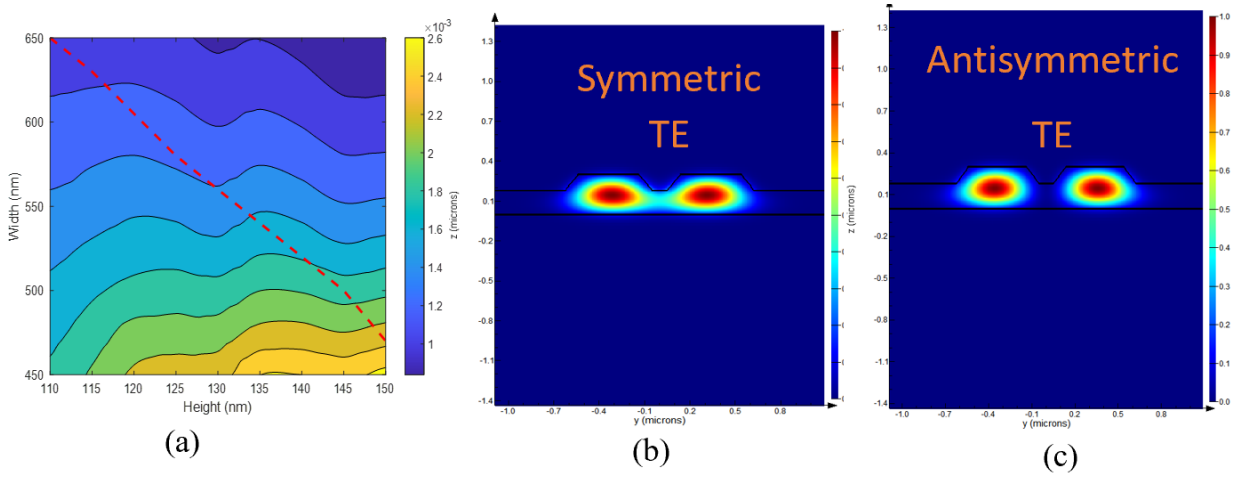

Fig. 2 (a) Variation of Δn_TE-Δn_TM with respect to width and etch depth of directional coupler. (b) The symmetric (c) and antisymmetric modes of the directional coupler for TE polarization

After optimizing the width and etch depth of waveguides, we designed an S-bend with minimal footprint and bending losses to obtain a compact polarization independent device. We varied the length of S-bend to make it loss less for TE and TM polarization (Fig. 3). We achieved 99% transmission efficiency for both TE and TM at 25 microns bending length for 10 microns of bend (Fig. 3). Such a polarization insensitive S-bend at low bending lengths can help enable compact photonic devices.

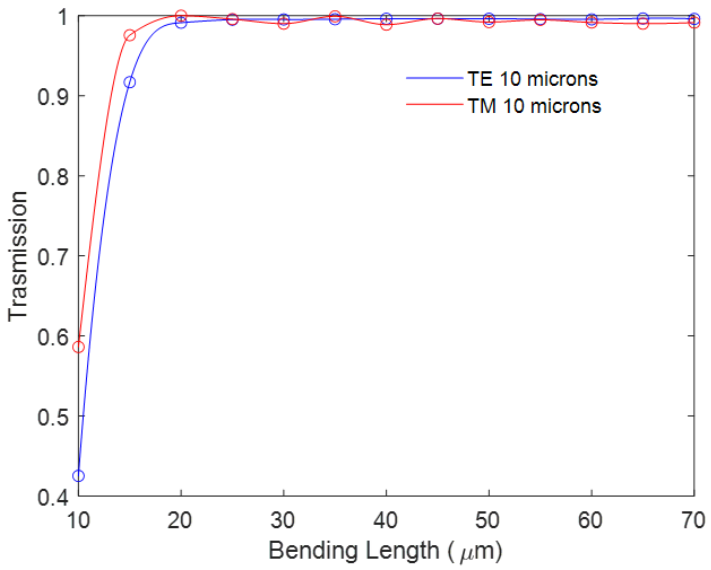

.

Fig. 3 Variation of the transmission coefficient with bending length for the optimization of the S-bend for TE and TM polarizations.

As the power splitting ratio of the directional coupler varies periodically with the coupling length (Lc), we then optimized the coupling length of the directional coupler to achieve a 50-50 coupling ratio for both TE and TM polarization (Fig. 4(a)). To achieve 50-50 coupling ration for TE and TM polarization, we minimize the quantity $\delta=(p1_{TE} + m_{TE}\ )2 + (p1_{TM} + m_{TM}\ )2$

(Fig. 4(b)) where $p1_{TE}$ and $p1_{TM}$ represents the power in waveguide 1 for TE and TM polarization and m_{TE} and m_{TM} represents the mean transmitted power of in waveguide 1 and waveguide 2 for TE and TM polarization respectively. Going through a higher order period of coupling length (75.5 microns coupling length), we achieved 50.2-49.2 (Fig.4(c)) and 51.2-47.85 (Fig, 4(d)) power splitting ratios for TE and TM, respectively. Apart from achieving 50-50 power splitting ratio, we can achieve any power splitting ratio independent of polarization which can be utilized to build quantum gates taking polarization degrees of freedom (Fig. 4(a)).

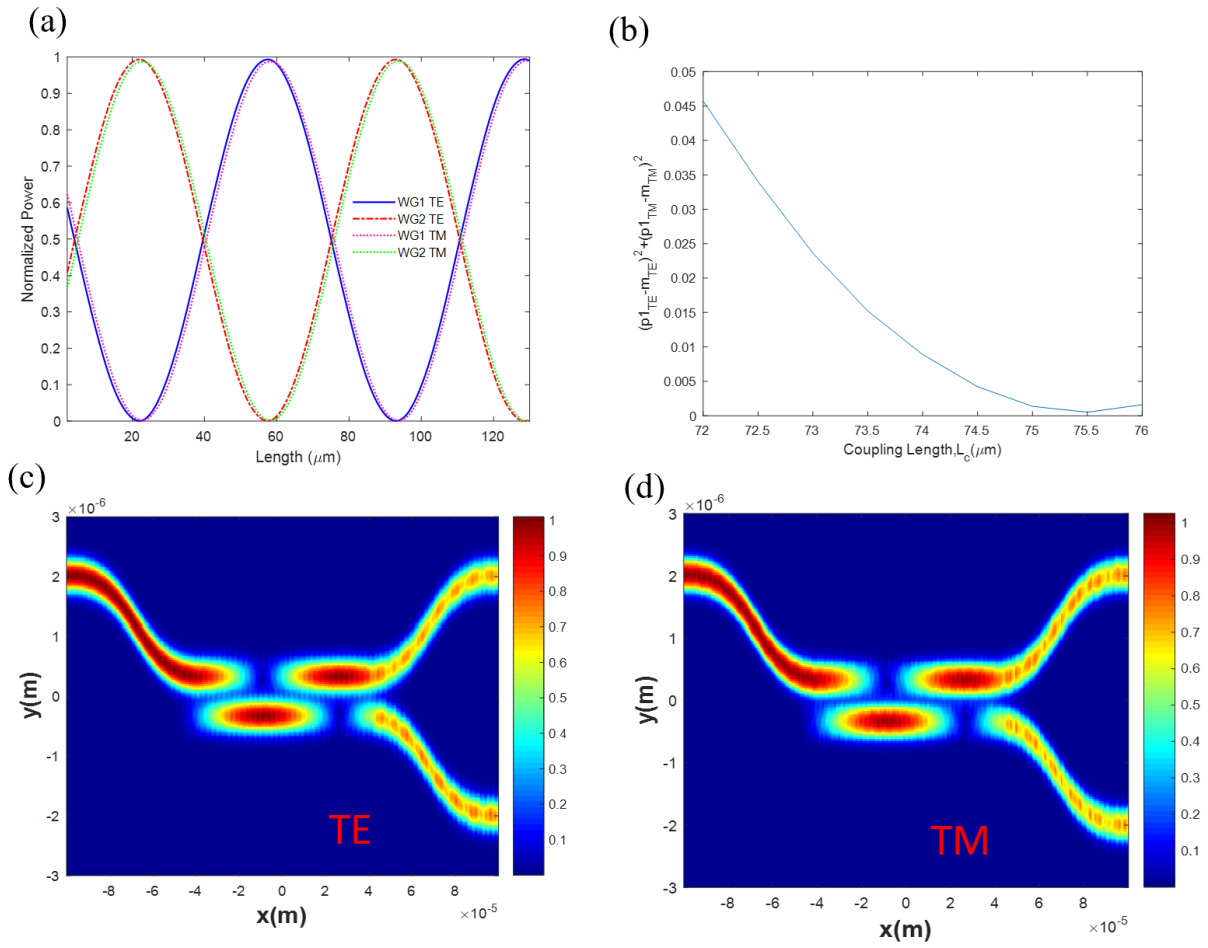

Fig. 4 (a) Periodic variation of normalized power splitting ratio of waveguide 1 and 2 with respect to coupling length for TE and TM polarization (b) Variation of δ with respect to coupling length to equalize power splitting ratio in waveguide 1 and 2 for TE and TM polarization (c) and (d) represent the electric field propagation through the directional coupler for TE and TM polarization respectively.

Finally, we analyzed the coupling efficiency that can be achieved through a lensed fiber of our designed directional coupler. For that reason, we compared the overlap of the integral of the waveguide mode and gaussian beam of the lensed fiber (Fig. 5(a) and 5(b)) to find the coupling efficiency from lensed fiber. We obtained 61% and 59% coupling efficiencies for TE and TM polarization, respectively (Fig. 5 (c)) at 0.6 numerical aperture (500 nm spot size of gaussian beam). Because of asymmetry of spot size, overlap integral decrease with increasing NA and waveguide without taper works better than tapered waveguide. Through our design, we can incorporate light in a polarization independent manner from a fiber to a chip.

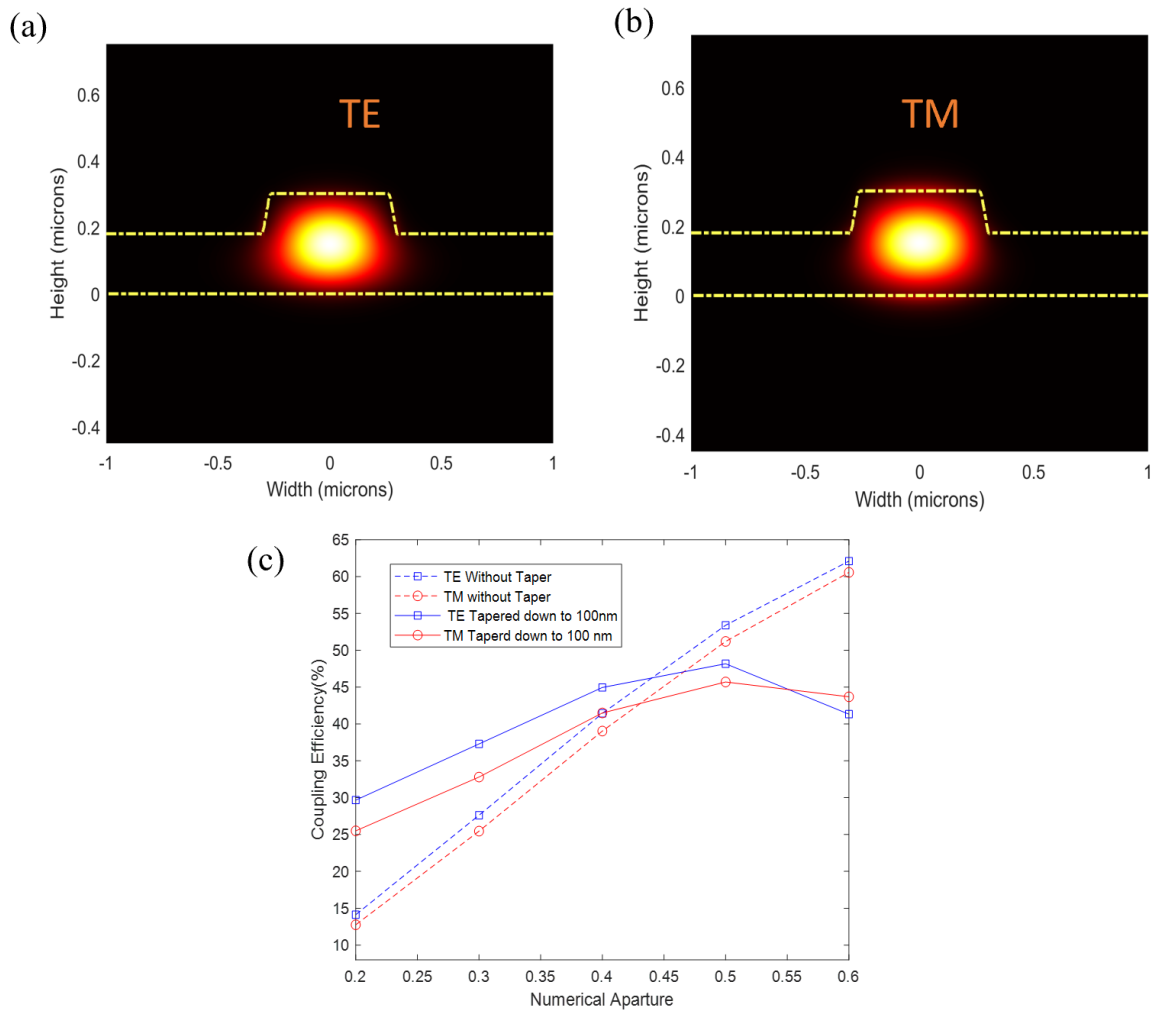

Fig. 5 (a) and (b) represents the electric field profile of waveguide for TE and TM polarization respectively and (c) plot of coupling efficiency from fiber to chip with respect to numerical aperture of lensed fiber

Grating coupler optimization

Grating couplers are used to couple light between free space and the ring resonators in our work. In order to maximize the detected signal from the ring resonators, we optimized the coupling efficiency of lithium niobate grating couplers at 493nm by sending a mode source into the waveguide and investigating the scattered light within 10 degrees from the grating coupler via FDTD simulations. As shown in figure (a), (b), we consider designs of grating couplers of size around 10 microns by 10 microns with a sidewall angle of 55 degrees, sitting in the middle of SiO_2 layers. By sweeping the period and fill factor in 3D simulations, we obtained the maximum

coupling efficiency of 4.64%, with 13.3% light scattered out and 34.8% of them within 10 degrees. The optimized design has a period of 440 nm and a fill factor of 0.8, with 22 periods in total and is going to be fabricated in the next step.

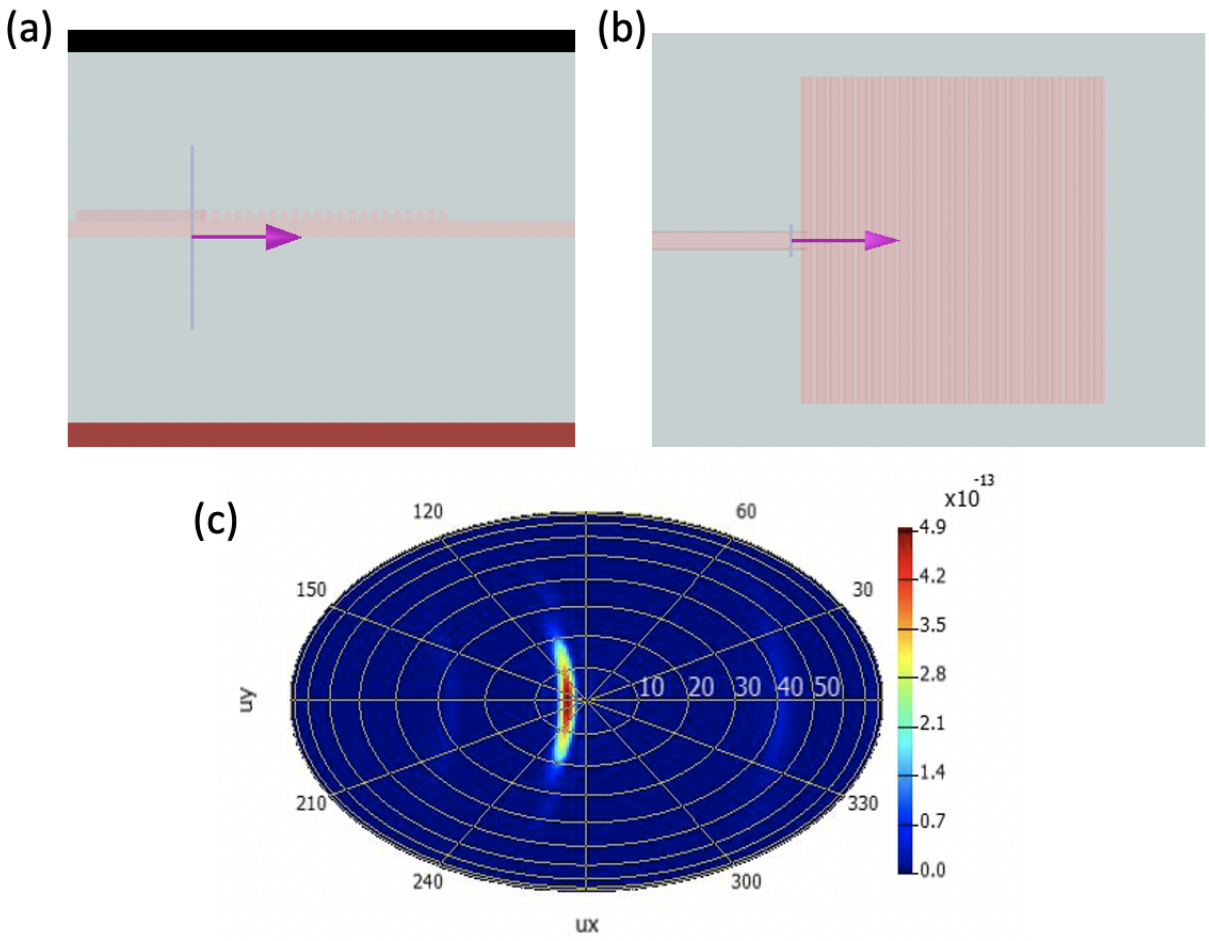

Fig. (a) Side view of the simulated grating coupler structure. A mode source is sent to the waveguide and the light scattered by the grating coupler is investigated. (b) Top view of the grating coupler. The grating coupler is around 10 microns by 10 microns. (c) Far field of the optimized design. Light is mostly scattered within an angle of 10 degrees.

Quantum frequency conversion

Distribution of quantum resources such as entanglement and qubits over a long distance through fiber optic network is the key for wide spread quantum communication. In recent years, trapped ions quantum information have achieved attention for scalable quantum computers for their high coherence time, high fidelity single and two qubit gates, straight forward state preparation and readout, fundamentally identical species and isotope etc. However, commonly used $^{171}Yb^{+}$ and

$^{138}Ba^{+}$ have major transitions at 369.53 nm and 493 nm which hinders them to send the quantum information over long distances because of the losses of fibers at visible wavelengths. For this reason, quantum frequency conversion is necessary to convert single photons emitted from ions into telecom photons which can be transmitted over a long distance. In this project, we are trying to convert single photons emitted from $^{138}Ba^{+}$ at 493 nm wavelength into telecom photons using nonlinearities of lithium niobate.

Quantum Frequency Conversion from 493 to 1530 nm

Quantum frequency conversion of single photons (SP) emitted by $^{138}Ba^{+}$ involves two steps as we reported in the previous year. In the first step, SP at 493 nm wavelength has been converted to 780 nm using 1343 nm pump laser through difference frequency generation (DFG) in periodically poled lithium niobate (PPLN). After that, 780 nm SP is being sent through the second PPLN and converted to 1530 nm SP using 1590 pump laser. In the previous year, we have achieved around 20% conversion efficiency in our first stage. This year, we have improved the conversion efficiency of the first stage by going free coupling. We discovered that the pigtailed was the main limitation behind conversion efficiency of the first stage(The attached figure below).

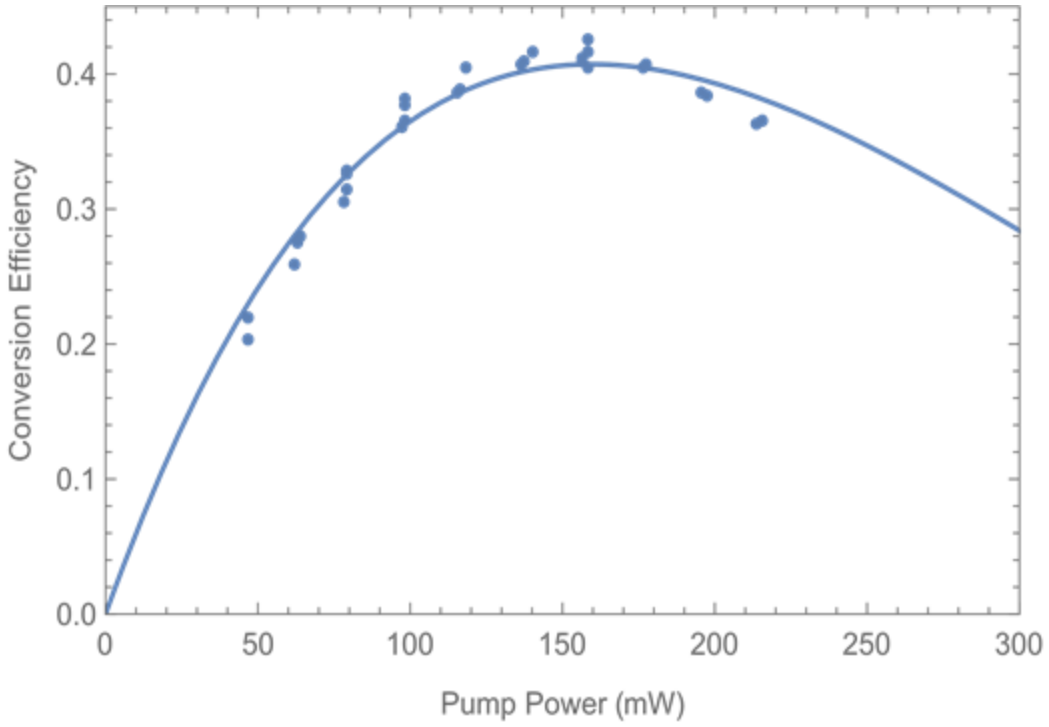

Figue: End to end conversion efficiency going from 493 nm single photons to 780 single photon using 1343 pump laser

We have tried to implement the second step of frequency conversion from 780 nm SP to 1530 nm SP using 1590 nm pump laser with PPLN provided by SRICO the last year. However, we are limited with poor conversion and high noise counts which forbids us to do single photon experiments. Therefore, we investigated the reason behind poor conversion efficiency and found that losses are coming from the pigtailed coupling which is not optimized for 1530 nm SP. Apart from that, the phase matching temperature and numerical aperture of PPLN waveguide wasn't provided by SRICO which makes the coupling of 780 nm light difficult.

For these reasons, we have shifted to directly bonded ridge PPLN waveguide provided by NTT electronics. The following figure represents the experimental set up of that.

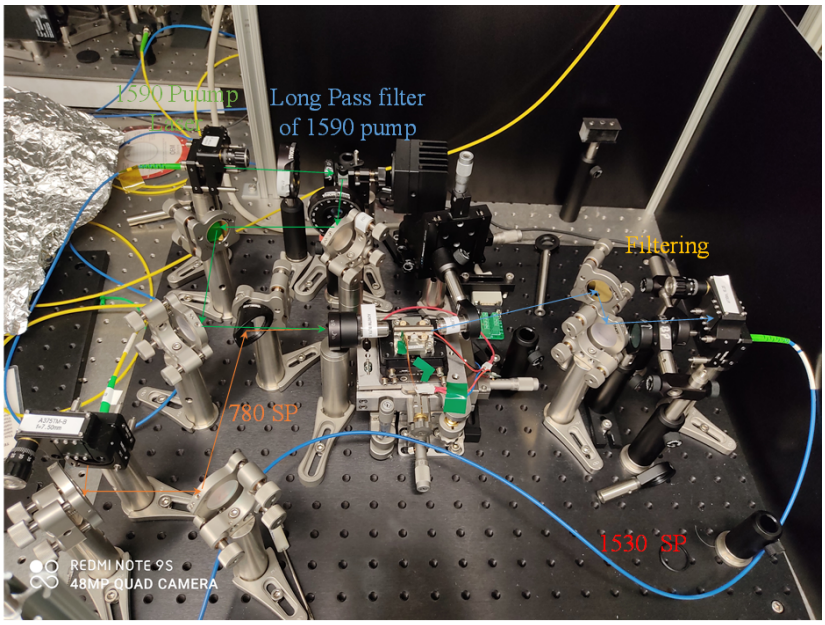

Figure: Our set up for converting 780 SP to 1532 nm SP using 1590 pump laser

Currently, we got 47% conversion efficiency in the second stage and the figure below represents the end to end coupling efficiencies with respect to pump power. In this experiment, we achieved the maximum conversion efficiency at 300 mW pump power which is lower than our previous experiment.

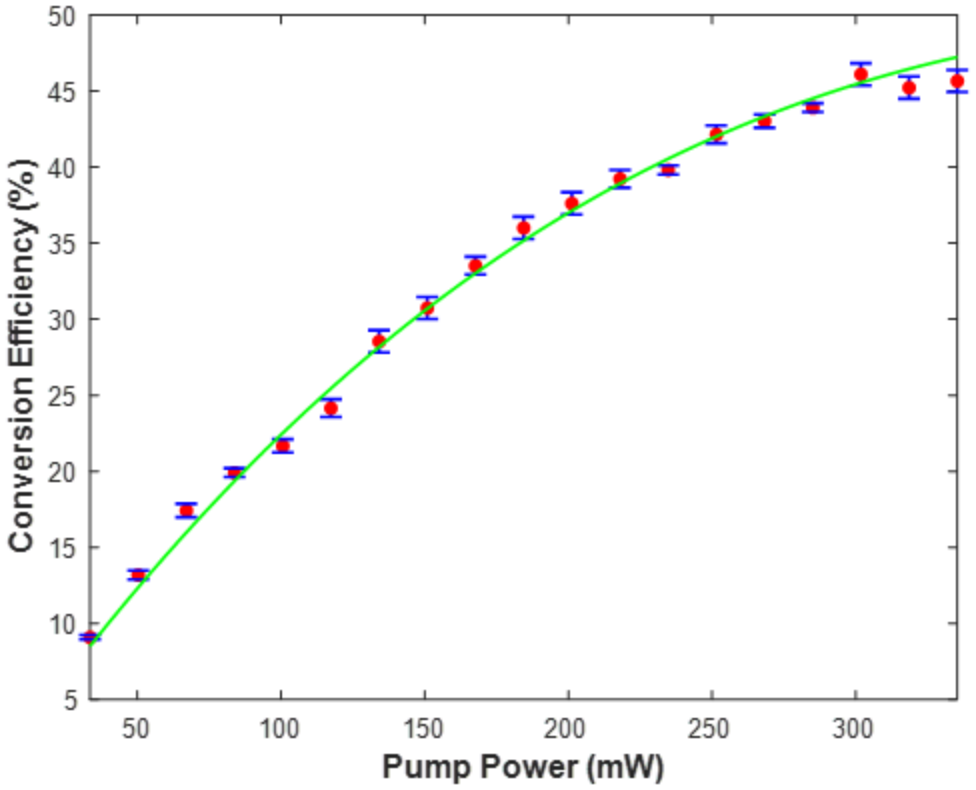

Fig. The end to end conversion efficiency of the second stage from 780 nm SP to 1530 SP photons vs 1590 nm pump power

To filter out the noise counts, we have used 3 nm spatial filtering followed by 20 GHz fiber bragg grating. However, we are getting 2 MHz noise counts because the idler is very close to the pump frequency for which raman scattering becomes the dominant noise. To filter the noise more, we have applied 50 MHz fabry perot filter and the noise spectrum of 1590 pump laser is shown below.

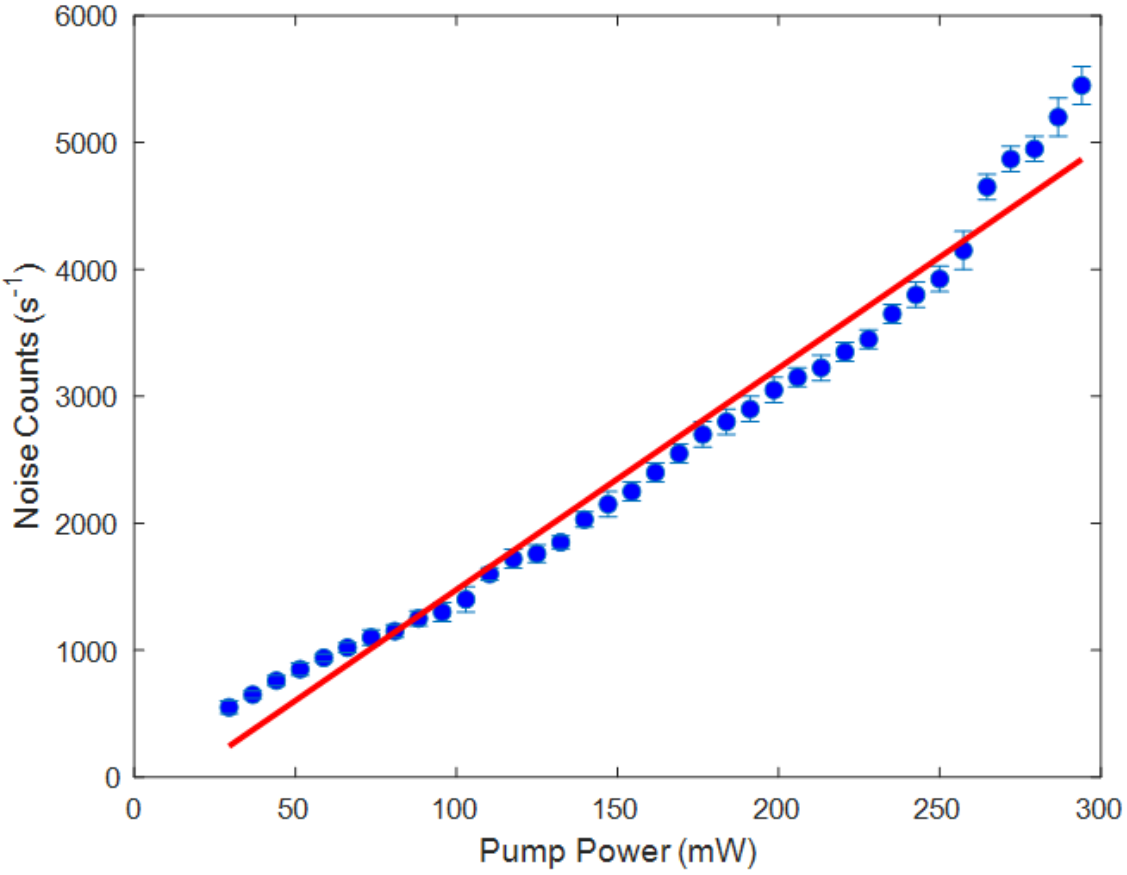

Figure : The noise counts after using 50 MHz filtering of 1590 pump laser used in converting 780 single photons to 1530 single photons.

Optical quantum memories for quantum networks

Quantum computing has picked up pace in recent times with several platforms at the forefront, like trapped ions and superconducting qubits. However, a full-scale quantum internet necessitates the ability to connect several different quantum computing nodes via quantum interconnects that preserve a quantum state over long distances. Photons are by far the medium of choice for developing quantum interconnects since they can utilize the vast network of optical fibers that is already laid out across the globe. However, a fundamental challenge to a distributed quantum computing network is the photon losses that are incurred in optical fibers. These losses limit the distribution of quantum entanglement to a length scale of only a few tens of kilometers. Quantum repeater nodes integrated with the fiber network system has been proposed to overcome this challenge. A vital cog in the proposed quantum repeater architectures is a quantum memory that can map quantum states encoded in photons on to matter and

establish entanglement distribution across two quantum nodes with high fidelity. Hence, a broadband quantum memory is the need of the hour to make significant progress towards a full-scale quantum internet.

As a vital step towards an integrated, tunable, broadband quantum memory, we have designed a new material consisting of rare earth ions (Thulium and Erbium) doped in thin film lithium niobate on insulator. The unique material stack allows for planar fabrication to realize strong light matter coupling of the ions with nanopatterned photonic structures. As a first step we have characterized the optical properties of the ions in the thin film to verify that they retain their favorable optical properties.

FIg. 1(A) compares the absorption through a 0.75 mm thin film waveguide and a 1 mm long bulk crystal. We show that both the transitions exhibit similar lineshapes and center wavelengths with an absorption coefficient of 14 cm^{-1} which is identical to the bulk absorption coefficient. Fig. 1(B) compares the photoluminescence emission from a bulk sample and a thin film waveguide. The exact agreement between the lineshapes and the inhomogeneous linewidths proves that the ion in the thin film do not experience additional stress due the the effects of the complex fabrication steps.

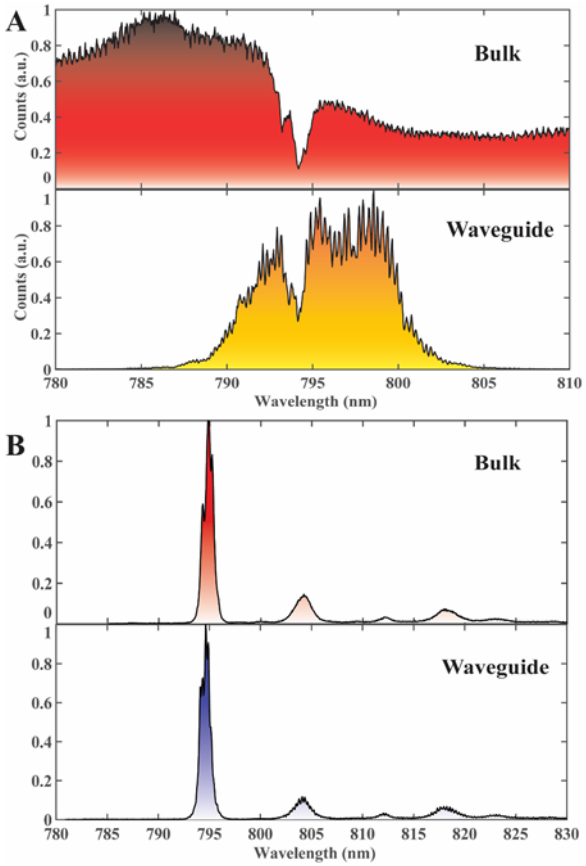

Fig. 1 (A) and (B) Shows the broadband absorption and photoluminescence through a bulk sample and a thin film waveguide respectively.

We performed time resolved photoluminescence experiments on the bulk sample and the fabricated waveguide as show in Fig. 2. The agreement between the extracted lifetimes of 160 μs demonstrates that the thin film ions do not experience any additional non-radiative decay mechanisms.

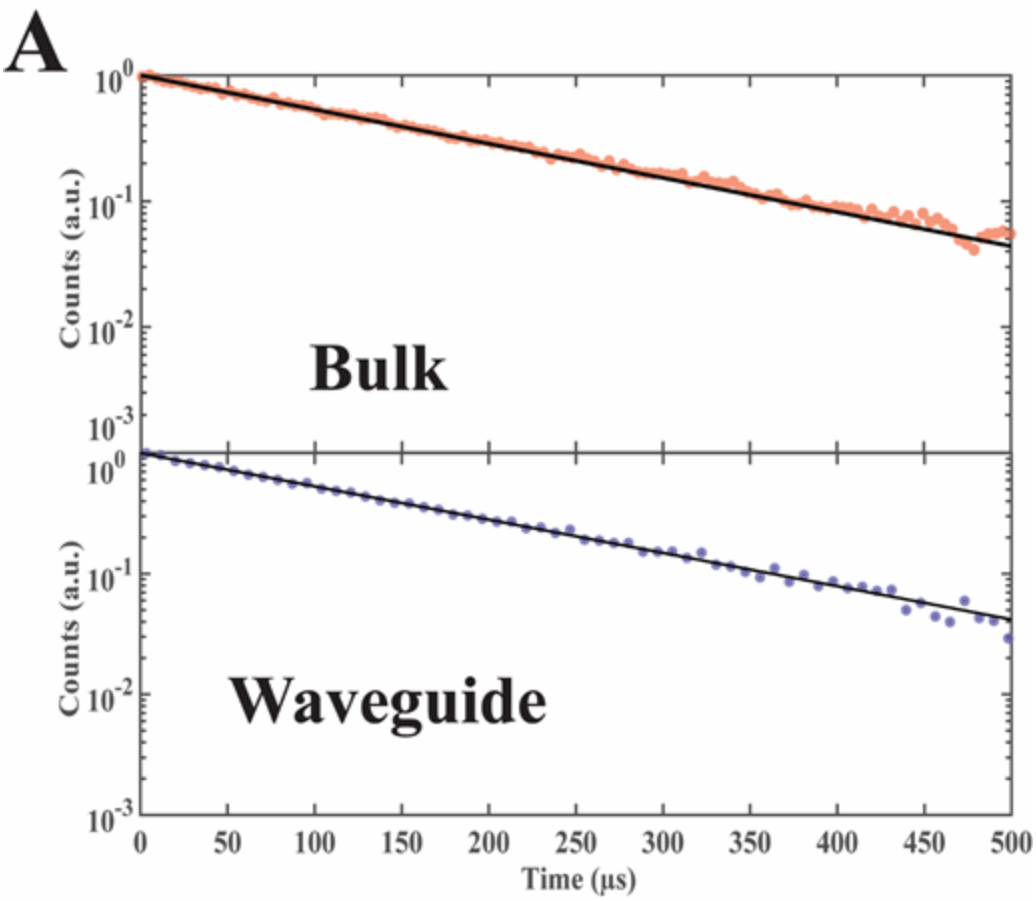

Fig. 2 (A) Time resolved photoluminescence measurements through the bulk and a thin film waveguide respectively.

The ability to burn narrow spectral holes is a key feature of rare earth ion ensembles that enables the realization of a broadband atomic frequency comb quantum memory. We demonstrate spectral hole burning, Fig. 3(A) in the thin film waveguides with powers of 10 nW, which is over three orders of magnitude lower than that previously reported in bulk ion diffused waveguides. We further verified in Fig. 3(B) that the spectral shapes of the hole are narrow with a linewidth of 1.6 MHz which is consistent with that reported in previously known bulk samples.

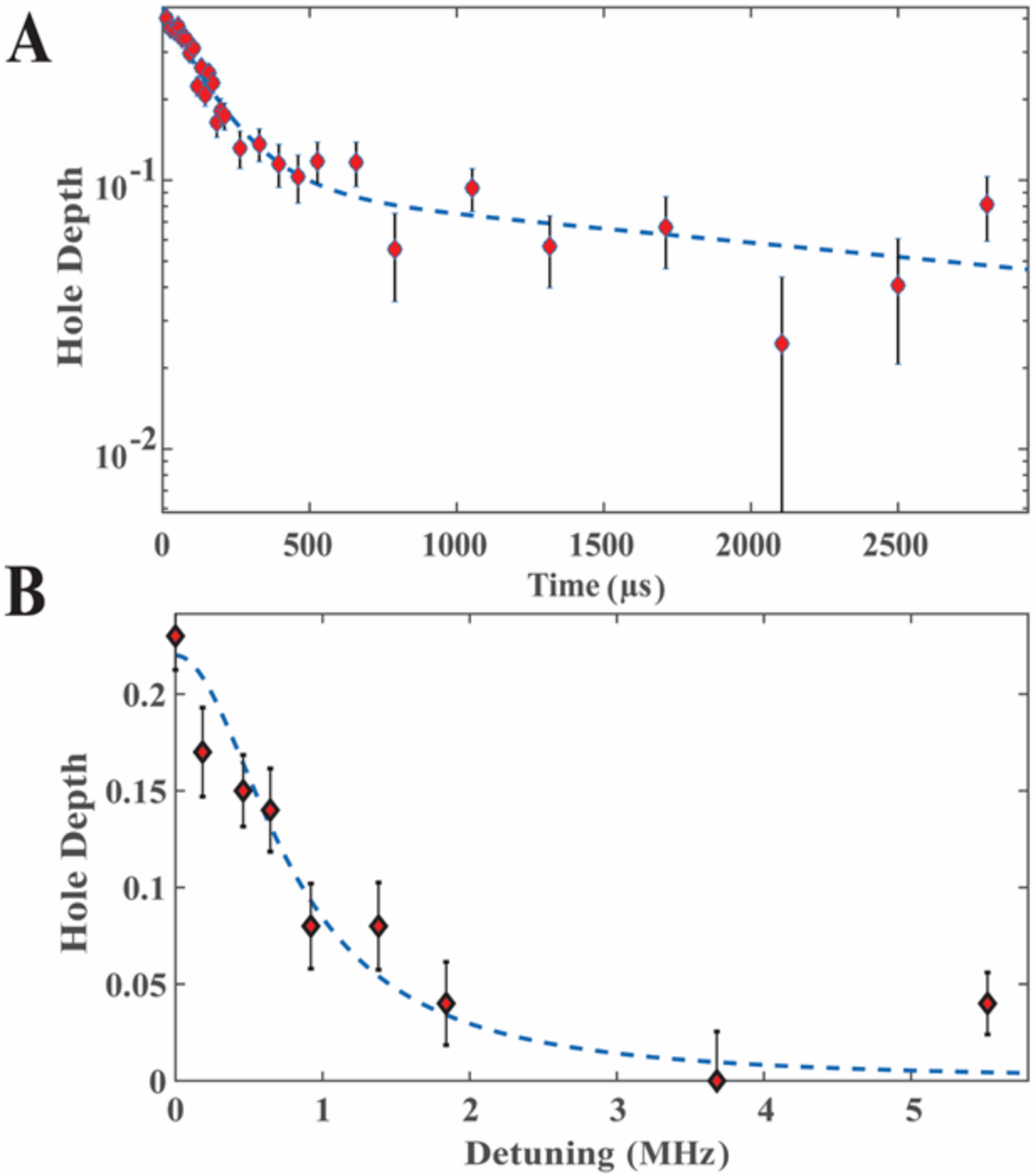

Fig 6 (A) Shows a time resolved spectral hole in a thin film waveguide. (B) Shows a frequency resolved spectral hole in a thin film waveguide.

Routing Single photons from ions with Photonic Integrated Circuits

Quantum networks require methods to route single photons between different network nodes. Integrated photonic devices offer a compact and scalable solution to this problem. These devices

can pack many components on a chip which can rapidly reconfigure themselves. Additionally, we can use photonic integrated circuits to multiplex single photons from different nodes and send it through the same channel, increasing the channel capacity. They can be also utilized as an optical cross connect switch for secure quantum communication and scaling up quantum computing and simulations. Therefore, to realize scalable quantum networks, it is essential to couple and route single photons from a stable quantum node using the photonic integrated circuits.

In this work, we demonstrate the routing of a single photon emitted from a trapped ion using a photonic integrated circuit. Trapped ions are excellent candidates for quantum networks because of their hour-long coherence time, high fidelity single- and two- qubit gates and the ability to generate single photons with ion's internal spin. However, they emit single photons in ultra-violet and visible regime making them incompatible for present day photonic foundry.

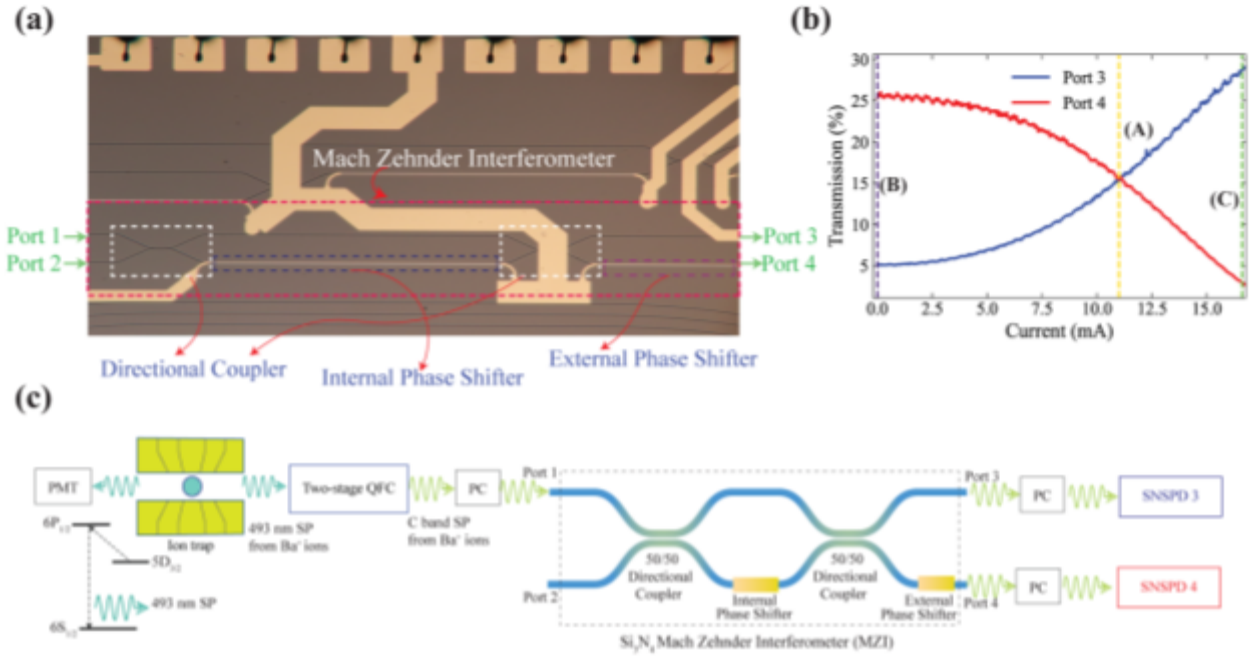

Fig. 1 (a) Optical microscope image of Mach-Zehnder interferometer fabricated on silicon nitride photonic platform. (b) Transmission characteristics of the output ports of Mach-Zehnder interferometer with current applied to internal phase-shifter. (c) Optical setup of coupling single photon from trapped ion to photonic integrated circuits. We use two-stage quantum frequency conversion (QFC) to generate C-band telecom photon from trapped ion. We couple the photons to SMF 28 fiber and connect them to polarization maintaining Fujikura 1550 fiber which is then edge-coupled to the chip (not shown in the diagram). Using free space polarization control (PC) stage consisting of half and quarter waveplate, we align the polarization of the single photons with TE-polarized waveguide. We use fiber arrays to couple and collect light from the chip (not shown in the diagram). We use polarization sensitive superconducting nanowire single-photon detector (SNSPD) to record the arrival time of the photon. Using photomultiplier tube (PMT) and time tagger, we construct the temporal photon shape of 493 nm photon collected from the other side of the trap.

For efficient coupling and routing, we generate C-band telecom single photons from a trapped barium ion using a two-stage quantum frequency conversion process (Fig. 1). We use a silicon-nitride Mach-Zehnder interferometer as a photonic router and switch the single photons to different output channels in a programmable way. By setting the Mach-Zehnder interferometer at a 50/50 splitting condition we can form an integral part of an on-chip Bell-state analyzer. This will be particularly advantageous as mode-profiles will be well matched in the waveguides resulting in high entanglement rate. Our demonstration opens new possibilities for scalable quantum networks where single photons emitted from stationary matter qubits can be routed and interfered to generate and herald entanglement between the nodes.

Generating O Band telecom photon from ion with high signal-to-noise ratio

In our new scheme, we are using two-stage quantum frequency conversion scheme to generate O band single photons from a trapped barium ion for long distanced quantum network. We are using ground state transition of $^{138}Ba^{+}$ ions to produce single photons at 493 nm wavelength. In our first stage, we are generating 780 nm single photons from 493 nm single photons using 1343 nm pump laser. We have replaced our previous second stage and currently generating 1283 nm single photons using 1989 nm pump laser. Our new second stage quantum conversion will boost the signal-to-noise ratio about three orders of magnitude from our previous experiment. Currently, we achieved 63.5% conversion efficiency of second stage quantum frequency conversion stage (Fig. 2).

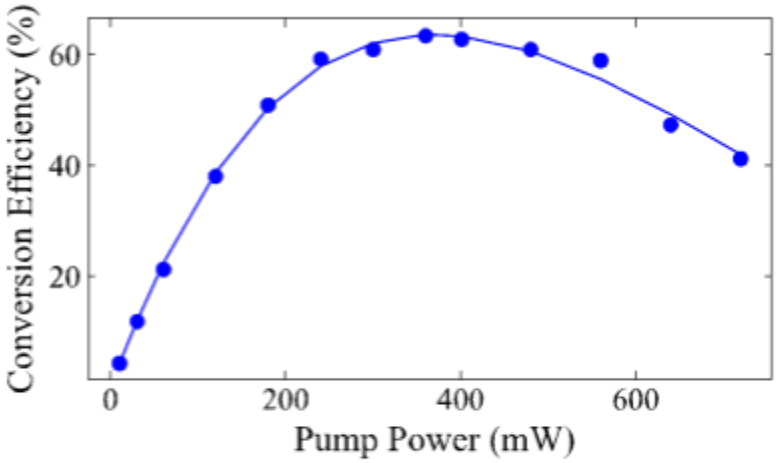

Fig. 2 Free space conversion efficiency of the second stage quantum frequency conversion going from 780 nm to 1283 nm using 1989 nm pump laser.

Publications

Dutta, Subhojit, Elizabeth A. Goldschmidt, Sabyasachi Barik, Uday Saha, and Edo Waks. 2020a. "Integrated Photonic Platform for Rare-Earth Ions in Thin Film Lithium Niobate." *Nano Letters* 20 (1): 741–47.

Dutta, Subhojit, Elizabeth Goldschmidt, Sabyasachi Barik, Uday Saha, and Edo Waks. 2020b. "A Scalable Nanophotonic Platform for Rare Earth Ions." *Bulletin of the American Physical Society* 65.

Dutta, Subhojit, Yuqi Zhao, Uday Saha, Demitry Farfurnik, Elizabeth A. Goldschmidt, and Edo Waks. 2022. "An Atomic Frequency Comb Memory in Rare-Earth Doped Thin-Film Lithium Niobate." In *CLEO: QELS_Fundamental Science*, FF3K – 7. Optica Publishing Group.

Hannegan, John, Uday Saha, James D. Siverns, Jake Cassell, Edo Waks, and Qudsia Quraishi. 2021. "C-Band Single Photons from a Trapped Ion via Two-Stage Frequency Conversion." *Applied Physics Letters* 119 (8): 084001.

Kwan, Michael, James Siverns, and Edo Waks. 2022. "A Modular Trapped Ion Node for Long Distance Quantum Networking." *Bulletin of the American Physical Society*.

Saha, Siverns, Hannegan, Prabhu, Bersin, Bandyopadhyay, Carolan, Quraishi, Englund, and Waks. n.d. "Integration of Single Photons from a Trapped Ion in a Programmable Photonic Circuit." *Bulletin of the American Physical Society*.

Saha, Siverns, Hannegan, Prabhu, Bersin, Bandyopadhyay, Carolan, Quraishi, Englund, and Waks. n.d. "Photonic Chip-Based Scalable Switching of Single Photons from a Trapped Ion." *Bulletin of the American Physical Society*.

Saha, Uday, John Hannegan, James Siverns, Jake Cassell, Edo Waks, and Qudsia Quraishi. 2021. "Telecom Single Photons from a Trapped Ba+ Ion." *Bulletin of the American Physical Society* 66.

Saha, Uday, James D. Siverns, John Hannegan, Mihika Prabhu, Eric Bersin, Saumil Bandyopadhyay, Jacques Carolan, Qudsia Quraishi, Dirk Englund, and Edo Waks. 2021. "Integration of Single-Photon from a Trapped Ion into a Photonic Chip." *Bulletin of the American Physical Society* 66.

Saha, Uday, James D. Siverns, John Hannegan, Mihika Prabhu, Eric Bersin, Saumil Bandyopadhyay, Jacques Carolan, Qudsia Quraishi, Dirk Englund, and Edo Waks. 2022. "Routing Single Photons from a Trapped Ion with Photonic Integrated Circuits." In *CLEO: QELS_Fundamental Science*, FTh5O – 1. Optica Publishing Group.

Saha, Uday, James D. Siverns, John Hannegan, Mihika Prabhu, Qudsia Quraishi, Dirk Englund, and Edo Waks. 2022. “Routing Single Photons from a Trapped Ion Using a Photonic Integrated Circuit.” *arXiv Preprint arXiv:2203. 08048*.

Saha, Uday, James Siverns, John Hannegan, Mihika Prabhu, Eric Bersin, Saumil Bandyopadhyay, Jacques Carolan, Qudsia Quraishi, Dirk R. Englund, and Edo Waks. 2022b. “Scalable Routing of Single Photons from a Trapped Ion on a Photonic Chip.” In *Optical Interconnects XXII*, PC120070E. SPIE.

Saha, Uday, and Edo Waks. 2021. “Design of an Integrated Bell-State Analyzer on a Thin-Film Lithium Niobate Platform.” *IEEE Photonics Journal* 14 (1): 1–9.

Saha, Uday, and Edo Waks. 2022. “A Polarization-Independent Directional Coupler on a Thin-Film Lithium Niobate Platform.” In *CLEO: Science and Innovations*, STh4H – 2. Optica Publishing Group.

Seshadreesan, Kaushik, Prajit Dhara, Norbert Linke, Edo Waks, and Saikat Guha. 2022. “Multiplexed Quantum Repeaters Based on Dual-Species Trapped-Ion Systems.” *Bulletin of the American Physical Society*.

Routing Single photons from ions with Photonic Integrated Circuits

Quantum networks require methods to route single photons between different network nodes. Integrated photonic devices offer a compact and scalable solution to this problem. These devices can pack many components on a chip which can rapidly reconfigure themselves. Additionally, we can use photonic integrated circuits to multiplex single photons from different nodes and send it through the same channel, increasing the channel capacity. They can be also utilized as an optical cross connect switch for secure quantum communication and scaling up quantum computing and simulations. Therefore, to realize scalable quantum networks, it is essential to couple and route single photons from a stable quantum node using the photonic integrated circuits.

In this work, we demonstrate the routing of a single photon emitted from a trapped ion using a photonic integrated circuit. Trapped ions are excellent candidates for quantum networks because of their hour-long coherence time, high fidelity single- and two- qubit gates and the ability to

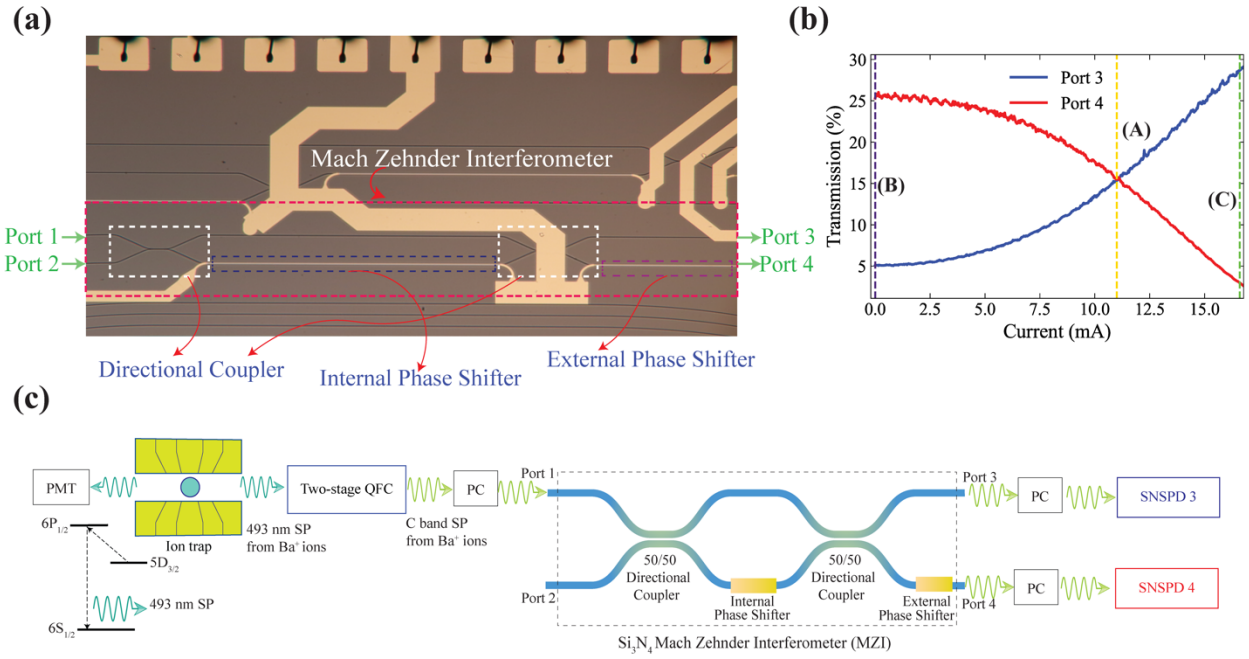

Fig. 1 (a) Optical microscope image of Mach-Zehnder interferometer fabricated on silicon nitride photonic platform. (b) Transmission characteristics of the output ports of Mach-Zehnder interferometer with current applied to internal phase-shifter. (c) Optical setup of coupling single photon from trapped ion to photonic integrated circuits. We use two-stage quantum frequency conversion (QFC) to generate C-band telecom photon from trapped ion. We couple the photons to SMF 28 fiber and connect them to polarization maintaining Fujikura 1550 fiber which is then edge-coupled to the chip (not shown in the diagram). Using free space polarization control (PC) stage consisting of half and quarter waveplate, we align the polarization of the single photons with TE-polarized waveguide. We use fiber arrays to couple and collect light from the chip (not shown in the diagram). We use polarization sensitive superconducting nanowire single-photon detector (SNSPD) to record the arrival time of the photon. Using photomultiplier tube (PMT) and time tagger, we construct the temporal photon shape of 493 nm photon collected from the other side of the trap.

generate single photons with ion's internal spin. However, they emit single photons in ultra-violet and visible regime making them incompatible for present day photonic foundry.
For efficient coupling and routing, we generate C-band telecom single photons from a trapped barium ion using a two-stage quantum frequency conversion process (Fig. 1). We use a silicon-nitride Mach-Zehnder interferometer as a photonic router and switch the single photons to different output channels in a programmable way. By setting the Mach-Zehnder interferometer at a 50/50 splitting condition we can form an integral part of an on-chip Bell-state analyzer. This will be particularly advantageous as mode-profiles will be well matched in the waveguides resulting in high entanglement rate. Our demonstration opens new possibilities for scalable quantum networks where single photons emitted from stationary matter qubits can be routed and interfered to generate and herald entanglement between the nodes.

Generating O Band telecom photon from ion with high signal-to-noise ratio

In our new scheme, we are using two-stage quantum frequency conversion scheme to generate O band single photons from a trapped barium ion for long distanced quantum network. We are using ground state transition of $^{138}Ba^{+}$ ions to produce single photons at 493 nm wavelength. In our first stage, we are generating 780 nm single photons from 493 nm single photons using 1343 nm pump laser. We have replaced our previous second stage and currently generating 1283 nm single photons using 1989 nm pump laser. Our new second stage quantum conversion will boost the signal-to-noise ratio about three orders of magnitude from our previous experiment. Currently, we achieved 63.5% conversion efficiency of second stage quantum frequency conversion stage (Fig. 2).

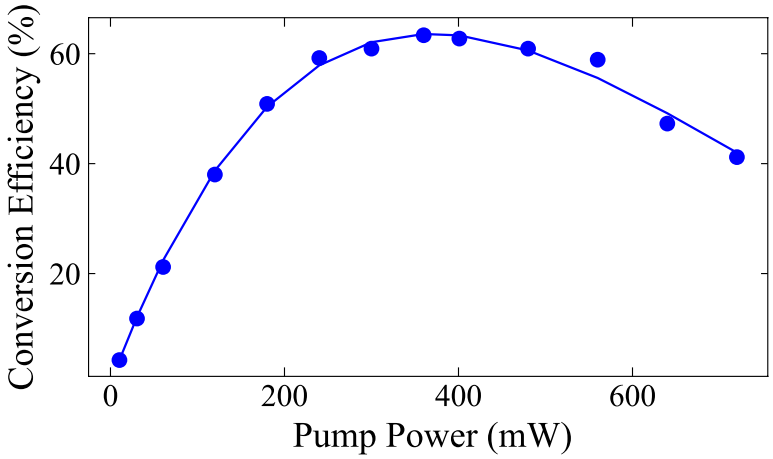

Fig. 2 Free space conversion efficiency of the second stage quantum frequency conversion going from 780 nm to 1283 nm using 1989 nm pump laser.